QUARTERLY OF APPLIED MATHEMATICS
VOLUME LXVII, NUMBER 3
SEPTEMBER 2009, PAGES 579–592
S 0033-569X(09)01157-X
Article electronically published on May 14, 2009

READILY COMPUTABLE GREEN'S AND NEUMANN FUNCTIONS FOR SYMMETRY-PRESERVING TRIANGLES

By

R. D. HAZLETT (*Potential Research Solutions, 1818 Shelmire Dr., Dallas, Texas 75224*)

AND

D. K. BABU (*Potential Research Solutions, 1818 Shelmire Dr., Dallas, Texas 75224*)

Abstract. Neumann and Green's functions of the Laplacian operator on 30-60-90° and 45-45-90° triangles can be generated with appropriately placed multiple sources/sinks in a rectangular domain. Highly accurate and easily computable Neumann and Green's function formulas already exist for rectangles. The extension to equilateral triangles is illustrated. In applications, closed-form expressions can be constructed for the potential, the streamfunction, or the various spatial derivatives of these properties. The derivation of analytic line integrals of these functions allows the proper handling of singularities and facilitates extended applications to problems on domains with open boundaries. Using a boundary integral method, it is demonstrated how one can construct semi-analytical solutions to problems defined on domains that exhibit spatially-dependent properties (heterogeneous media) or possess irregular boundaries.

1. Introduction. Green's and Neumann functions of the Laplacian operator are commonly used to give analytical representations of solutions to boundary value problems in fluid convection, heat conduction, and electromagnetics. Highly accurate, fast computing solutions are available for rectangular domains of an arbitrary length-to-width aspect ratio [12]. The use of boundary integral methods to produce a patchwork of coupled analytic solutions for the potential in systems of heterogeneous transport properties in two and three dimensions has already been demonstrated [6]. The same methodology was extended to semi-analytic solutions in the form of a streamfunction for 2-D applications [7]. Such fast-computing Neumann function formulas were used to define the objective function in optimization schemes for real applications, such as the placement

Received July 2, 2008.
2000 *Mathematics Subject Classification.* Primary 35A20; Secondary 35B60, 35C05.
Key words and phrases. Neumann function, Green's function, right triangle, boundary integral method.
This work was supported by grants from the National Science Foundation's Small Business Innovation Research Program, Contracts DMI-0128291 and DMI-0236569. Any opinions, findings, and conclusions or recommendations expressed in this material are those of the authors and do not necessarily reflect the views of the National Science Foundation.
E-mail address: rdhazlett@sbcglobal.net

©2009 Brown University
Reverts to public domain 28 years from publication

of oil and gas wells in hydrocarbon reservoirs to maximize well productivity or fractional recovery.

The method of images was seen to be particularly useful in the development of time-dependent Neumann solutions to the heat equation for 3-D rectangular regions [15]. As possible solution building blocks to address problems on nonrectangular domains, Green's and Neumann functions for triangles are of particular interest [1, 3, 9, 13]. Efforts to produce infinite series of image mappings for arbitrary right triangles have proven elusive, as the symmetry-breaking problem has scuttled attempts to formulate closed-form solutions for all but special case right triangles [8]. Figure 1 is a photo taken from behind an internally illuminated triangular chamber with walls made of two-way mirrors, allowing one to visualize sources inside the chamber and the infinite set of reflections generated by those sources. This chamber corresponds to a right triangle with acute angles unevenly divisible into 360°. As such, the reflection pattern contains countless symmetry-breaking events. This loss of symmetry tremendously compounds the difficulty in formulating an infinite sequence describing the location of sources in imaginary space required to construct Green's and Neumann functions for triangles by the method of images. However, for 30-60-90° and isosceles right (45-45-90°) triangles, matching sets of infinite images were found for equivalent multiple source rectangle problems. The nontrivial extension of these results yields Green's and Neumann functions for the equilateral triangle (60-60-60°), important in a number of natural gridding problems. In this paper, we describe the development of highly accurate, easily computed Neumann function formulas on these special case triangles, then demonstrate their use in a mixed-domain, boundary integral problem.

2. Results. We show that the Green's and Neumann functions for an isosceles right triangle, $N_{\triangle}(x, y; x_o, y_o)$, are generated from the corresponding two-source problem on a unit square by locating a point source at (x_o, y_o) and its mirror image across the diagonal at (y_o, x_o). Similarly, the Neumann function problem for a 30-60-90° triangle, $N_{\triangle}(x, y; x_o, y_o)$, with right angle at $(a, 0)$ and the longer leg on the x-axis, is generated by a corresponding rectangle problem with 6 sources of equal strength inside a rectangle with base, a, and height, $b = a\sqrt{3}$. If the original source location is (x_o, y_o) interior to the triangle, additional image sources of equal strength magnitude, μ_i, are placed at:

$$x_1 = \frac{1}{2}(x_o + \sqrt{3}y_o), y_1 = \frac{1}{2}(\sqrt{3}x_o - y_o); \tag{2.1}$$

$$x_2 = \frac{1}{2}(x_o - \sqrt{3}y_o), y_2 = \frac{1}{2}(\sqrt{3}x_o + y_o); \tag{2.2}$$

$$x_3 = a - x_2, y_3 = a\sqrt{3} - y_2; \tag{2.3}$$

$$x_4 = a - x_1, y_4 = a\sqrt{3} - y_1; \tag{2.4}$$

$$\text{and} \quad x_5 = a - x_o, y_5 = a\sqrt{3} - y_o. \tag{2.5}$$

This last result is found to be analogous to Prager's [16] prolongation of the symmetric part of a function for the Laplace operator on an equilateral triangle, which uses reflections, rotations, and translations to reformulate the problem. An analogous path

FIG. 1. Reflections of source objects (ruler, candle, illuminated box, and light bulb) in a 34-56-90° triangular chamber composed of two-way mirrors. A portion of the real chamber is seen in the foreground. At each acute angle vertex, the space-filling images fail to construct an integer number of chamber reflections and objects therein. This loss of symmetry poses a significant mathematical challenge to the methods of images.

to the Green's and Neumann function formulas for an equilateral triangle is demonstrated which makes use of a mixed-boundary solution representing the skew-symmetric case. Using the fast computing, closed-form Green's and Neumann function formulas of McCann *et al.* [12], the Laplace solution on such special case triangles for potential can be readily evaluated for either Dirchlet or Neumann boundary conditions. Where the Neumann function is used for illustration purposes, the Green's function could be likewise constructed by alternating sources and sinks, i.e. by changing the sign on the strength magnitude upon each reflection.

It is further demonstrated that a boundary element problem can be posed and solved with the continuity of $\Phi(x)$ and the normal derivative, $\partial\Phi/\partial n$, across open boundaries of special case right triangles. An example is provided for a potential mapped across a flow field involving a source and sink in communication across a shared boundary between a square and an isosceles right triangle.

3. Development.

3.1. *Rectangular systems.* The Green's and Neumann functions for the Laplacian operator on the rectangle $0 \leq x \leq a$, $0 \leq y \leq b$, with the singularity located at (x_o, y_o), are

given by Duff and Naylor [4]:

$$G(x,y;x_o,y_o) = \frac{4}{\pi^2 ab}\sum_{m,n=1}^{\infty} \frac{\sin(\frac{m\pi x}{a})\sin(\frac{m\pi x_o}{a})\sin(\frac{n\pi y}{b})\sin(\frac{n\pi y_o}{b})}{\frac{m^2}{a^2}+\frac{n^2}{b^2}}, \tag{3.1}$$

$$N(x,y;x_o,y_o) = \frac{4}{\pi^2 ab}\sum_{m,n=0}^{\infty} C_{mn}\frac{\cos(\frac{m\pi x}{a})\cos(\frac{m\pi x_o}{a})\cos(\frac{n\pi y}{b})\cos(\frac{n\pi y_o}{b})}{\frac{m^2}{a^2}+\frac{n^2}{b^2}}, \tag{3.2}$$

respectively, where $C_{00}=0$, $C_{m0}=C_{0n}=0.5$, and $C_{mn}=1$ for $m>0, n>0$. The periodicity of the source locations on the RHS of (3.1) and (3.2) illustrates the influence of the infinite number of images of the original source across the boundaries of the rectangle.

McCann *et al.* [12] showed that the above slowly convergent double infinite series for the Neumann function could be replaced by a highly accurate approximation. For $b \geq a$,

$$N(x,y;x_o,y_o) = \frac{1}{\pi}\sum_{m=1}^{M}\frac{f_m e^{-2m\pi b/a}}{m(1-e^{-2m\pi b/a})} + h(y,y_o) + \delta_M$$
$$-\frac{1}{4\pi}\sum_{i=1}^{4}\ln[(1+E_i^2-2E_i\cos(\frac{\pi}{a}(x-x_o)))(1+E_i^2-2E_i\cos(\frac{\pi}{a}(x+x_o)))], \tag{3.3}$$

where

$$f_m = \cos(\frac{m\pi x}{a})\cos(\frac{m\pi x_o}{a})(E_1^m+E_2^m+E_3^m+E_4^m), \tag{3.4}$$

$$h(y,y_o) = \frac{b}{a}(\frac{1}{3}-\frac{\max(y,y_o)}{b}+\frac{y^2+y_o^2}{2b^2}), \tag{3.5}$$

$$\text{and}\quad |\delta_M| \leq \frac{2}{\pi}\sum_{m=M+1}^{\infty}\frac{e^{-2m\pi b/a}}{m(1-e^{-2m\pi b/a})} \tag{3.6}$$

$$\text{with}\quad E_1 = e^{-\pi(y+y_o)/a},\qquad E_3 = e^{-\pi(2b-(y+y_o))/a},$$
$$E_2 = e^{-\pi|y-y_o|/a},\qquad E_4 = e^{-\pi(2b-|y-y_o|)/a}. \tag{3.7}$$

If $b<a$, the variables should be transposed. McCann *et al.* [12] obtained the equivalent of formulas (3.3)–(3.7) as the two-dimensional version of the solution to a three-dimensional heat equation problem in anisotropic porous media derived by Babu and Odeh [2] to study oil production from a horizontal well, identified as a finite length line sink. Others have independently sought Green's and Neumann solutions for the Laplacian operator on the rectangle [10, 11, 17].

For practical applications, the sum of the logarithmic terms and the ramp function, h, of (3.3) is an excellent approximation to the exact solution. The finite sum to M terms, involving the f_m function above, denotes *correction terms* and may require at most $M \leq 2$ terms for the worst case, a square ($a=b$). For $b>a$, the accuracy increases rapidly. An estimation of the maximum absolute error is given by (3.6). For a square ($a=b$), for $M=0,1,2,etc.$, $|\delta_M| < 1.191\times10^{-3}, 1.110\times10^{-6}, 1.382\times10^{-9}$, *etc.*

3.2. *Symmetry-preserving right triangles.* A physical model was constructed to study mirror image propagation throughout space in triangular systems [8]. Representations of the infinite set of source images by easily computable infinite series proved elusive for all but special case right triangles, as illustrated in Figure 1. Patterns for right triangles

which could be tiled onto infinite space are diagrammed in Figure 2. By inspection and simple algebra, it was determined that an identical reflection pattern would result from an appropriate arrangement of multiple sources in a rectangular box unit cell. The new rectangular and original triangular unit cells are highlighted in Figure 2. The identification of the isosceles right triangle problem with an equivalent square problem is accomplished with a single fold across the diagonal. The identity of a 30-60-90° triangle problem with a $(1 \times \sqrt{3})$ rectangular unit cell problem requires five folds or five mirrored copies of the original triangle. As such, closed form solutions to the Laplacian operator for these special right triangles in two dimensions can be readily constructed using the basic expressions of (3.3) or suitable derivatives thereof.

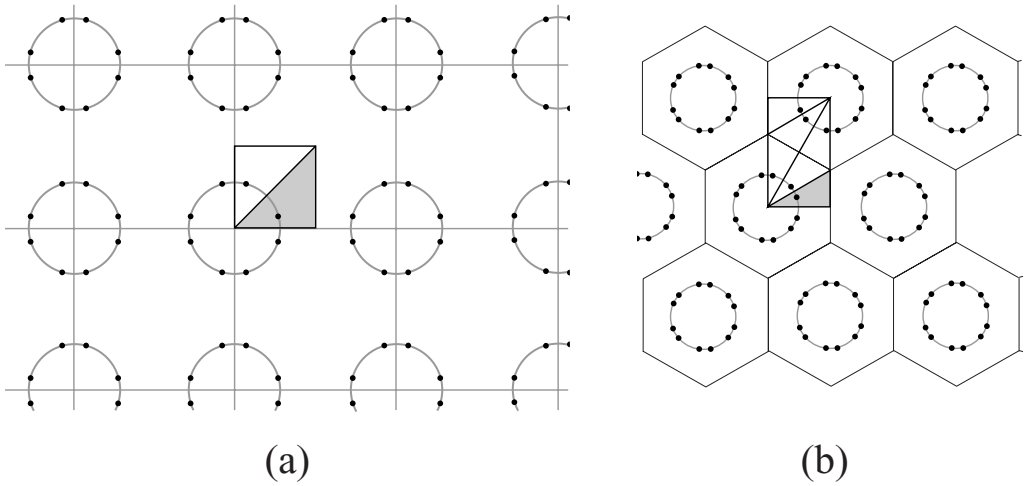

FIG. 2. Source reflections in symmetry-preserving triangles: (a) an isosceles right triangle, and (b) a 30-60-90° triangle. Since the Neumann function is derived for a point source, orientation is not at issue. The original triangle is shown in gray, while the unit cell is outlined in black. Note the circular repeating unit, with diameter and source distribution determined by the source location within real space, on a grid of spacing determined by the folding of the unit cell.

The Neumann function for the isosceles right triangle with leg, a, in terms of the Neumann function for the square (see (3.2) with $a = b$) obtained from a single fold across the diagonal is thus

$$N_{\triangle}(x,y;x_o,y_o) = \frac{4}{\pi^2}\sum_{m,n=0}^{\infty} C_{mn}\frac{\cos(\frac{\pi m x}{a})\cos(\frac{\pi n y}{a})}{m^2+n^2} \times \left[\cos\left(\frac{\pi m y_o}{a}\right)\cos\left(\frac{\pi n x_o}{a}\right) + \cos\left(\frac{\pi m x_o}{a}\right)\cos\left(\frac{\pi n y_o}{a}\right)\right]. \tag{3.8}$$

Similarly, the Neumann function for the 30-60-90° triangle in terms of a rectangle with base, a, and height, $b = a\sqrt{3}$, is

$$N_{\triangle}(x,y;x_o,y_o) = \frac{4\sqrt{3}}{\pi^2}\sum_{m,n=0}^{\infty} C_{mn}\frac{\cos(\frac{\pi mx}{a})\cos(\frac{\pi ny}{b})}{3m^2+n^2} \times \left[\sum_{i=0}^{5}\cos\left(\frac{\pi mx_i}{a}\right)\cos\left(\frac{\pi ny_i}{b}\right)\right], \tag{3.9}$$

where the additional source terms (x_i, y_i) are given in (2.1)–(2.5).

Although algebraic manipulations may be employed to show that the normal flux across the hypotenuse of the 30-60-90° triangle vanishes, from a heuristic point of view, this could be inferred by noticing that following two reflections, the hypotenuse coincides with a portion of the rectangular boundary which clearly satisifes the Neumann boundary condition (see Figure2b).

Figure 3 gives maps of the potential and the streamfunction on a dense grid for a matched source and sink pair within flow domains given by isosceles right triangles (a–c) and 30-60-90° triangles (d–f). Figures 3(a,b,d,e) correspond to Neumann boundary conditions, while Figures 3(c,f) correspond to Dirichlet conditions on the triangle boundary for the same source/sink pair. Although only one triangle depicted within each image constitutes real space, mapping across the entire rectangular unit cell is shown for completeness. Streamfunction images illustrate particularly well the segmentation of the solution space into noninteracting reflected units of the original triangle.

3.3. *Extension to the equilateral triangle.* Prager [16] gave a prolongation method in which signs on sources in the rectangular unit cell for the 30-60-90° triangle are manipulated to form symmetric and skew-symmetric parts. In our reduction method, each formulation satisfies the Laplacian on the rectangle. The sum of solutions is also a solution, with the added benefit that the sum honors the desired boundary conditions on the equilateral triangle not present in the individual components. Both Green's and Neumann function formulas for the equilateral triangle are composed in such a manner. In both cases, the symmetric contribution is exactly that posed for the Green's or Neumann function for the 30-60-90° triangle. The skew-symmetric contribution is a mixed boundary solution, with Neumann boundary conditions on one set of parallel boundaries of the rectangle and Dirchlet conditions on the other. This corresponds to one set of boundary conditions on the short leg and hypotenuse of the 30-60-90° triangle with the other applied to the longer leg. An example of a Neumann function construction for the potential within the equilateral triangle is shown in Figure 4, where the summation effectively reduces the number of sources/sinks in the unit cell from six to three.

3.4. *Boundary integral method application.* Hazlett and Babu [6] used the Neumann function formulas with the operator $-(k_x\partial^2/\partial x^2 + k_y\partial^2/\partial y^2)$ by scaling the spatial variables $x' \equiv x/\sqrt{k_x}$, $y' \equiv y/\sqrt{k_y}$, where k_x and k_y represent anisotropic transport properties, to solve optimal well-positioning problems in two dimensions. Using the relationship between the potential and the streamfunction, Hazlett *et al.* [7] further developed objective functions making use of parameters extracted from both solution representations in optimal well-performance methodology. Calculation methods using

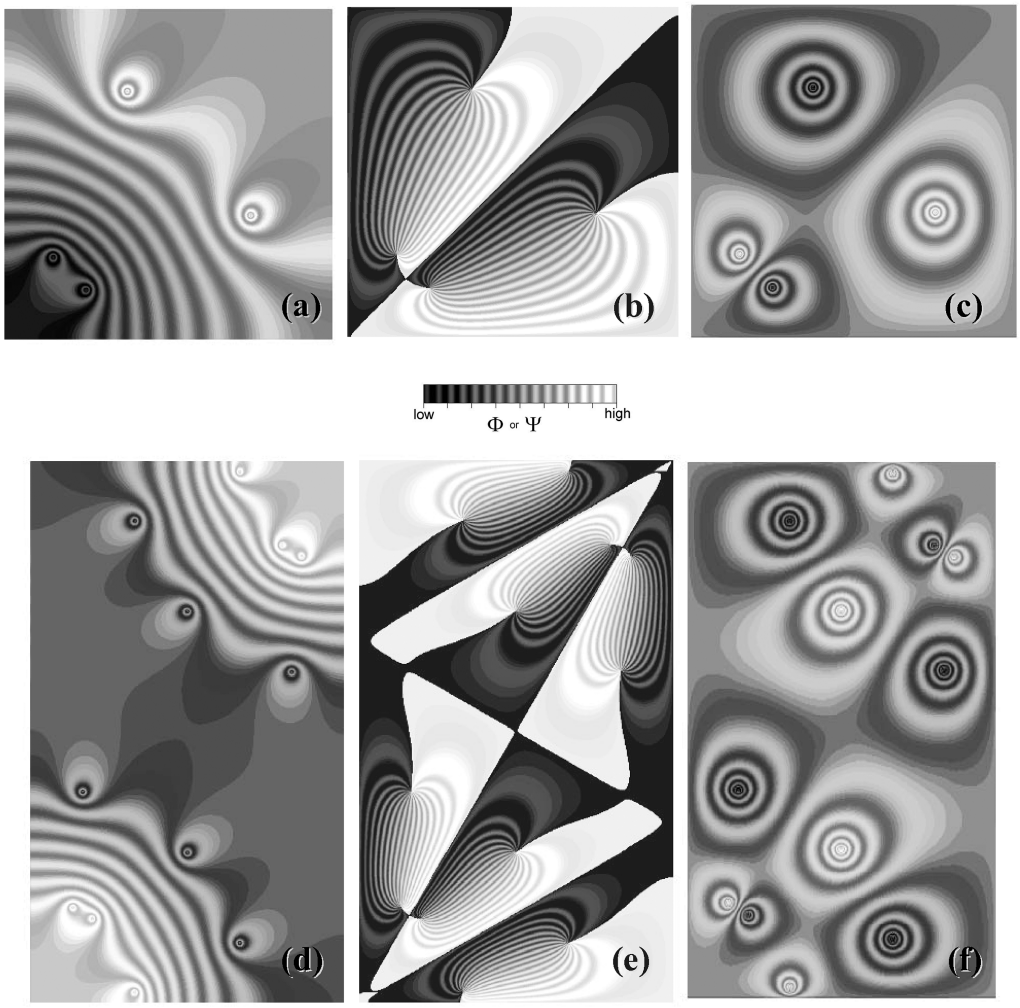

FIG. 3. Maps of the potential and the streamfunction with one source and one sink: (a) potential for the right isosceles triangle with Neumann boundary conditions, (b) streamfunction for the isosceles right triangle with Neumann boundary conditions, (c) potential for the right isosceles triangle with Dirichlet boundary conditions, (d) potential for the 30-60-90° triangle with Neumann boundary conditions, (e) streamfunction for the 30-60-90° triangle with Neumann boundary conditions, (f) potential for the 30-60-90° triangle with Dirichlet boundary conditions. Images show that the Neumann function for the triangular element is derived from the Neumann function on a larger parent rectangle with multiple sources. Sources are spaced to exactly replicate the infinite set of image sources generated by the triangle. The internal no-flow boundaries are apparent in the segmented streamfunction.

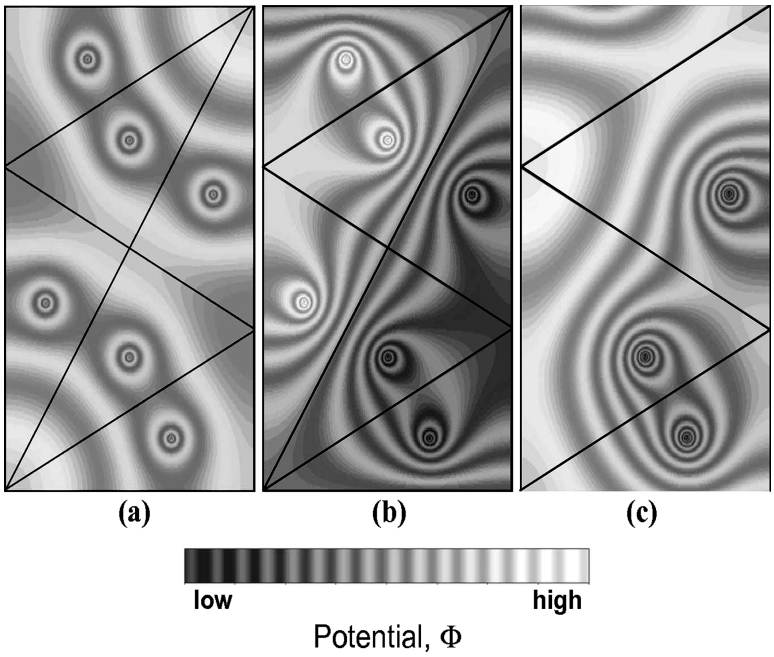

FIG. 4. Maps of the potential in Neumann function construction for the equilateral triangle: (a) potential for the symmetric case on the 30-60-90° triangle with Neumann boundary conditions, (b) potential for the skew-symmetric case on the 30-60-90° triangle with Neumann boundary conditions on x and Dirichlet conditions on y, (c) the sum of the symmetric and skew-symmetric cases, yielding the desired result on the equilateral triangle with Neumann boundary conditions and a single source.

fast computing Neumann formulas were extended to address open (porous) boundary problems by posing and solving boundary integral problems. As such, a network of coupled analytic solutions can tile a solution space of an irregular shape or spatially-varying transport properties.

In constructing boundary integral expressions, the proper handling of singularities in the Neumann function is essential. The expression to evaluate the potential, Φ, at an arbitrary point, $\vec{x}$, in open systems (nonzero flux, $g(\vec{\sigma})$, across parts of the boundary) for a source located at an interior point, $\vec{x_o}$, with strength $\mu = q/q_o$ is given as

$$\Phi(\vec{x}, \vec{x_o}) = \overline{\Phi} - \mu N(\vec{x}, \vec{x_o}) - \frac{1}{q_o} \int_S N(\vec{x}, \vec{\sigma}) g(\vec{\sigma}) d\sigma. \tag{3.10}$$

Next, considering boundary locations for $\vec{x}$, we get equivalently,

$$\Phi(\vec{x}, \vec{x_o}) = \overline{\Phi} - \mu N(\vec{x}, \vec{x_o}) - \frac{1}{q_o} \int_S N(\vec{x}, \vec{\sigma}) (g(\vec{\sigma}) - g(\vec{x})) d\sigma - \frac{g(\vec{x})}{q_o} \int_S N(\vec{x}, \vec{\sigma}) d\sigma. \tag{3.11}$$

Here, $d\sigma$ is a boundary element, $\vec{x}$ and $\vec{\sigma}$ are both point locations on the common boundary, S, $\overline{\Phi}$ is the average potential, N is the Neumann function, q_o is a reference production rate, S is the open interval boundary, and g is the surface normal flux.

In heterogeneous systems, (3.10) and (3.11) are used to establish continuity of the potential (pressure), $\Phi(\vec{x}, \vec{x_o})$, across two contiguous media using the Neumann function expressions appropriate for each region. In such cases, the normal flux, $g(\vec{\sigma})$, remains an unknown to be determined in an integral equation. Since $N(\vec{x}, \vec{\sigma})$ exhibits singular behavior at $\vec{x} = \vec{\sigma}$, (3.11) will facilitate numerical calculations. The singularity at $\vec{x} = \vec{\sigma}$ is neutralized within the first integration of (3.11). Analytic integration of the basic function, $N(\vec{x}, \vec{\sigma})$, in the last term successfully captures the singular portion. In the Appendix, we show the integration of the Neumann function along the boundaries of rectangles and special right triangles ((A-6), (A-8), (A-11), (A-20)). For a rectangle, integrating along the boundary $y = b$:

$$\int_0^a N(x, b; x_o, b) dx_o = b/3. \tag{3.12}$$

For an isosceles right triangle, integrating $N_{\triangle}(x, y; x_o, y_o)$ along one of the sides, $y = 0$, we have:

$$\int_0^a N_{\triangle}(x, 0; x_o, 0) dx_o = \frac{a}{6}\left[1 + 3\Big(1 - \frac{x}{a}\Big)^2\right]. \tag{3.13}$$

For a 30-60-90° triangle with longer side, a, integration of $N_{\triangle}(x, y; x_o, y_o)$ yields:

$$\text{Along longer side:} \quad \int_0^a N_{\triangle}(x, 0; x_o, 0) dx_o = \frac{a\sqrt{3}}{2}\Big(1 - \frac{x}{a}\Big)^2, \tag{3.14}$$

$$\text{Along shorter side:} \quad \int_0^{b/3} N_{\triangle}(a, y; a, y_o) dy_o = a\left[\frac{2}{9} + \frac{1}{2}\Big(\frac{y}{a}\Big)^2\right]. \tag{3.15}$$

With these constructs, pressure matching conditions at shared boundaries between regions of different shapes or transport properties can be posed in terms of the unknowns: g and $\overline{\Phi}$. Partial integration representations of (3.12)–(3.15) are likewise possible, but the resulting closed-form expressions are considerably more complex and not included here.

Using this logic and adding the appropriate conservation constraints, analytic solutions can be decoupled by solving the linear matrix equation set for normal flux distribution and average property value. An example is provided in Figure 5 for the potential mapped across a flow field involving a source and sink in communication across a shared boundary between a square and isosceles right triangle with Neumann external boundary conditions. The fictitious upper triangle used to form the Neumann function is plotted to portray problem symmetry, but the solution is valid for flow confined by the solid black boundary.

An equivalent development can proceed for Dirichlet boundary conditions for full or partially shared boundaries. The extension of special case triangle Neumann functions is straightforward for 3-D prisms with triangular cross section in the manner of Babu and Odeh [2].

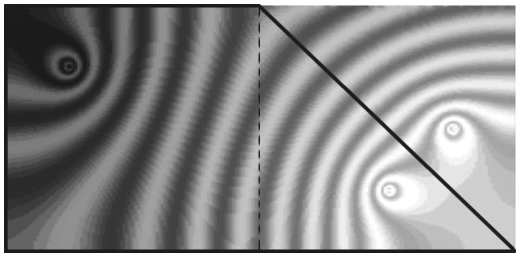

FIG. 5. An advanced application for a solution to the Laplace equation for collages of shapes, each with an analytical Neumann function. For such composite flow fields, continuation in potential and normal flux is guaranteed by a boundary element method. Boundary integrals (3.12) and (3.13) were used in handling the singularity at the boundary nodes for this problem.

Appendix.

A-1. Identities. We make use of the following identities [5]:

$$\sum_{n=1}^{\infty} \frac{\cos(\pi n x)}{n^2} = \pi^2 \left(\frac{1}{6} - \frac{x}{2} + \frac{x^2}{4} \right), \quad 0 \le x \le 2, \tag{A-1}$$

$$\sum_{n=1}^{\infty} \frac{\sin(\pi n x)}{n^3} = \pi^3 \left(\frac{x}{6} - \frac{x^2}{4} + \frac{x^3}{12} \right), \quad 0 \le x \le 2, \tag{A-2}$$

and for noninteger values of β:

$$\sum_{n=1}^{\infty} \frac{\cos(\pi n x)}{n^2 - \beta^2} = \frac{1}{2\beta^2} - \frac{\pi}{2\beta} \frac{\cos(\pi\beta(1-x))}{\sin(\pi\beta)}, \quad 0 \le x \le 2, \tag{A-3}$$

$$\sum_{n=1}^{\infty} \frac{(-1)^n \cos(\pi n x)}{n^2 - \beta^2} = \frac{1}{2\beta^2} - \frac{\pi}{2\beta} \frac{\cos(\pi\beta x)}{\sin(\pi\beta)}, \quad -1 \le x \le 1. \tag{A-4}$$

A-2. Boundary integrals for rectangular domains with Neumann boundary conditions. We seek the integral of the Neumann function along a rectangular domain boundary, with both the source, (x_o, y_o), and the observation point, (x, y), brought to the boundary at either $y = 0$ or $y = b$. Selecting the $y = b$ option, we rewrite (3.2) as

$$\int_0^a N(x, b; x_o, b) dx_o = \frac{4}{\pi^2 ab} \int_0^a \sum_{m,n=0}^{\infty} C_{mn} \frac{\cos(\pi m x/a) \cos(\pi m x_o/a)}{\frac{m^2}{a^2} + \frac{n^2}{b^2}} dx_o \tag{A-5}$$

The only nonzero term in the above integral is the single series contribution ($m = 0$)

$$I = \int_0^a N(x, b; x_o, b) dx_o = \frac{2}{\pi^2 ab} \int_0^a \sum_{n=1}^{\infty} \frac{b^2}{n^2} dx_o = \frac{b}{3}. \tag{A-6}$$

A-3. Boundary integral for the isosceles right triangle with Neumann boundary conditions. For the Neumann function for the isosceles right triangle, given as (3.8), the boundary integral on $[0,a]$ and $y=y_o=0$ is given by

$$\int_0^a N_{\triangle}(x,0;x_o,0)dx_o = \frac{4}{\pi^2}\int_0^a \sum_{m,n=0}^{\infty} C_{mn}\frac{\cos(\pi mx/a)}{m^2+n^2}\Big[\cos\Big(\frac{\pi mx_o}{a}\Big)+\cos\Big(\frac{\pi nx_o}{a}\Big)\Big]dx_o. \tag{A-7}$$

Again, only the single series contribute nonzero terms, yielding

$$I=\int_0^a N_{\triangle}(x,0;x_o,0)dx_o = \frac{2a}{\pi^2}\left[\sum_{m=1}^{\infty}\frac{1}{m^2}\cos\Big(\frac{\pi mx}{a}\Big)+\sum_{n=1}^{\infty}\frac{1}{n^2}\right] = \frac{a}{6}\left[1+3\Big(1-\frac{x}{a}\Big)^2\right]. \tag{A-8}$$

A-4. Boundary integral for the 30-60-90° triangle with Neumann boundary conditions.

A-4.1. *Line integral along longer leg.* Setting $y=y_o=0$ and $b=a\sqrt{3}$ in (3.9) and integrating along the base, $0\le x_o\le a$, yield

$$I=\frac{4\sqrt{3}}{\pi^2}\sum_{m,n=0}^{\infty}\int_0^a C_{mn}\frac{\cos\Big(\frac{\pi mx}{a}\Big)[1+\cos(\pi m)\cos(\pi n)]}{3m^2+n^2} \times\Big[\cos\Big(\frac{\pi mx_o}{a}\Big)+2\cos\Big(\frac{\pi mx_o}{2a}\Big)\cos\Big(\frac{\pi nx_o}{2a}\Big)\Big]dx_o. \tag{A-9}$$

Integrating and simplifying,

$$I=\frac{4\sqrt{3}}{\pi^2}\sum_{m,n=0}^{\infty}C_{mn}\frac{\cos\Big(\frac{\pi mx}{a}\Big)[1+\cos(\pi m)\cos(\pi n)]}{3m^2+n^2} \times\left[c+\frac{1}{\pi}\frac{2a}{m+n}\sin\left(\frac{\pi(m+n)}{2}\right)+\frac{1}{\pi}\frac{2a}{m-n}\sin\left(\frac{\pi(m-n)}{2}\right)\right]. \tag{A-10}$$

Here $c=\int_0^a\cos\Big(\frac{\pi mx_o}{a}\Big)dx_o=a$ when $m=0$ and zero for $m\neq 0$. The only nonzero terms arise from the two cases: the single series in n ($m=0$) and the limiting case where $m=n$. Hence,

$$I=\frac{2a\sqrt{3}}{\pi^2}\sum_{n=1}^{\infty}\frac{1+\cos(\pi n)}{n^2}+\frac{8a\sqrt{3}}{\pi^2}\sum_{n=1}^{\infty}\frac{\cos\Big(\frac{\pi nx}{a}\Big)}{4n^2} = \frac{a\sqrt{3}}{2}\Big(1-\frac{x}{a}\Big)^2. \tag{A-11}$$

A-4.2. *Line integral along shorter leg.* Setting $x = x_o = a$ and integrating along the short leg of the 30-60-90° triangle, $[0, b/3]$,

$$\begin{aligned} I &= \int_0^{b/3} N_{\triangle}(a, y; a, y_o) dy_o \\ &= \frac{4\sqrt{3}}{\pi^2} \sum_{m,n=0}^{\infty} \int_0^{b/3} C_{mn} \frac{\cos(\pi m)\cos(\pi n y/b)}{3m^2 + n^2} \\ &\quad \times \{[\cos(\pi m) + \cos(\pi n)] \cos\left(\frac{\pi n y_o}{b}\right) + 2\cos\left[\frac{\pi m}{2}(1 + \frac{3y_o}{b})\right] \cos\left[\frac{\pi n}{2}(1 - \frac{y_o}{b})\right] \\ &\quad + 2\cos[\frac{\pi m}{2}(1 - \frac{3y_o}{b})] \cos[\frac{\pi n}{2}(1 + \frac{y_o}{b})]\} dy_o. \end{aligned} \tag{A-12}$$

Integration and simplification gives

$$\begin{aligned} I = &\frac{4\sqrt{3}}{\pi^2} \sum_{m,n=1}^{\infty} \frac{\cos(\pi m)\cos\left(\frac{\pi n y}{b}\right)}{3m^2 + n^2} \left[\frac{b}{\pi n}[\cos(\pi m) + \cos(\pi n)] \sin\left(\frac{\pi n}{3}\right) \right. \\ &\left. + \frac{4bn}{\pi(n^2 - 9m^2)} \left(\sin\left(\frac{2\pi n}{3}\right) - \cos(\pi m)\sin\left(\frac{\pi n}{3}\right)\right)\right] \\ &+ I_o(n = 0) + I_o(m = 0), \end{aligned} \tag{A-13}$$

where I_o represents the single series results. Using partial fraction decomposition for the denominator term, $[(n^2 + 3m^2)(n^2 - 9m^2)]$, and simplifying,

$$\begin{aligned} I = &\frac{12\sqrt{3}b}{\pi^3} \sum_{m,n=1}^{\infty} \frac{\cos\left(\frac{\pi n y}{b}\right)}{n(n^2 - 9m^2)} \left[\sin\left(\frac{2\pi n}{3}\right)\cos(\pi m) - \sin\left(\frac{\pi n}{3}\right)\right] \\ &+ I_o(n = 0) + I_o(m = 0). \end{aligned} \tag{A-14}$$

Summing over m first in the double series and using $(\beta \to n/3)$ as a limiting case, using (A-3) and (A-4), we get

$$\begin{aligned} I = &\frac{6\sqrt{3}b}{\pi^3} \sum_{n=1}^{\infty} \frac{1 + \cos(\pi n)}{n^3} \left[\sin\left(\frac{\pi n}{3}\right)\cos\left(\frac{\pi n y}{b}\right)\right] \\ &+ \frac{2b\sqrt{3}}{\pi^2} \sum_{n=1}^{\infty} \frac{\cos\left(\frac{\pi n}{3}\right)\cos\left(\frac{\pi n y}{b}\right)}{n^2} + I_o(n = 0) + I_o(m = 0). \end{aligned} \tag{A-15}$$

The single series from (A-13):

$$I_o(n=0) = \frac{2\sqrt{3}}{\pi^2}\sum_{m=1}^{\infty}\int_0^{b/3}\frac{\cos(\pi m)}{3m^2}\left[1+\cos(\pi m)+4\cos\left(\frac{\pi m}{2}\right)\cos\left(\frac{3\pi m y_o}{2b}\right)\right]dy_o$$

$$= \frac{b\sqrt{3}}{54}, \tag{A-16}$$

$$I_o(m=0) = \frac{2\sqrt{3}}{\pi^2}\sum_{n=1}^{\infty}\int_0^{b/3}\frac{\cos\left(\frac{\pi n y}{b}\right)}{n^2}\left[[1+\cos(\pi n)]\cos\left(\frac{\pi n y_o}{b}\right)\right. \tag{A-17}$$

$$\left.+4\cos\left(\frac{\pi n}{2}\right)\cos\left(\frac{\pi n y_o}{2b}\right)\right]dy_o$$

$$= -\frac{6b\sqrt{3}}{\pi^3}\sum_{n=1}^{\infty}\frac{\cos\left(\frac{\pi n y}{b}\right)\sin\left(\frac{\pi n}{3}\right)[1+\cos(\pi n)]}{n^3}. \tag{A-18}$$

Combining (A-15), (A-16), and (A-18) finally gives

$$I = \frac{2b\sqrt{3}}{\pi^2}\sum_{n=1}^{\infty}\frac{\cos\left(\frac{\pi n y}{b}\right)\cos\left(\frac{\pi n}{3}\right)}{n^2} + \frac{b\sqrt{3}}{54}$$

$$= b\sqrt{3}\left(\frac{2}{27}+\frac{y^2}{2b^2}\right). \tag{A-19}$$

Since $b = a\sqrt{3}$,

$$I = a\left[\frac{2}{9}+\frac{1}{2}\left(\frac{y}{a}\right)^2\right]. \tag{A-20}$$

References

[1] H. Ahmedov and I. H. Duru, *Regularized Green's function and group of reflections in a cavity with triangular cross section*, Phys. Atom. Nucl., **68** (2005), 1621–1624.

[2] D. K. Babu and A. S. Odeh, *Productivity of a horizontal well*, SPE Reservoir Eng., November (1989), 417–421.

[3] R. Chadha and K. C. Gupta, *Green's functions for triangular segments in planar microwave circuits*, IEEE Trans. Microwave Theory Tech., **28** (1980), 1139–1143.

[4] G. F. D. Duff and D. Naylor, *Differential equations of applied mathematics*, Wiley, New York, NY, 1966. MR0192675 (33:900)

[5] I. M. Gradshteyn and I. M. Ryzhik, *Table of integrals, series, and products*, Corrected and enlarged edition, Academic Press, San Diego, CA, 1980, pp. 39–40. MR0582453 (81g:33001)

[6] R. D. Hazlett and D. K. Babu, *Optimal well placement in heterogeneous reservoirs through semi-analytic modeling*, SPE J., **10** (2005), 286–296.

[7] R. D. Hazlett, D. K. Babu, and L. W. Lake, *Semianalytical stream-function solutions on unstructured grids for flow in heterogeneous media*, SPE J., **12** (2007), 179–187.

[8] R. D. Hazlett, D. K. Babu, V. Chodur, S. Cook, and L. W. Lake, *A mirror on the world: Undergraduate researchers advance physics in triangular spaces*, *submitted to Journal of Engineering Education* (2009).

[9] M. E. Johnston, J. C. Myland, and K. B. Oldham, *A Green function for the equilateral triangle*, Z. Angew. Math. Phys., **56** (2005), 31–44. MR2112839 (2005h:35004)

[10] C. M. Linton, *Rapidly convergent modified Green's function for Laplace's equation*, Proc. R. Soc. Lond. A, **455** (1999), 1767–1797. MR1701551 (2000c:65097)

[11] S. L. Marshall, *A rapidly convergent modified Green's function for Laplace's equation in a rectangular region*, Proc. R. Soc. Lond. A, **455** (1999), 1739–1766. MR1701550 (2000d:65237)

[12] R. C. McCann, R. D. Hazlett, and D. K. Babu, *Highly accurate approximations of Green's and Neumann functions*, Proc. R. Soc. Lond. A, **457** (2001), 767–772. MR1875306 (2002j:76113)
[13] B. J. McCartin, *Eigenstructure of the equilateral triangle, part II: The Neumann problem*, Math. Probl. Eng., **8** (2002), 517–539. MR1967479 (2004j:35063)
[14] J. N. Newman, *The Green function for potential flow in a rectangular channel*, J. Engrg. Math., **26** (1992), 51–59. MR1154227 (92j:76009)
[15] A. S. Odeh and D. K. Babu, *Transient flow behavior of horizontal wells: Pressure drawdown and buildup analysis*, SPE Formation Eval., March (1990), 7–15.
[16] M. Prager, *Eigenvalues and eigenfunctions of the Laplace operator on an equilateral triangle*, Appl. Math., **43** (1998), 311–320. MR1627985 (99c:35036)
[17] J. Strain, *Fast potential theory. II. Layer potentials and discrete sums*, J. Comput. Phys., **99** (1992), 251–270. MR1158209 (93b:65197)